Membrane Transport, Structure, Function, and Biogenesis:

Shank2 Associates with and Regulates Na^+/H^+ Exchanger 3

WonSun Han, Kyung Hwan Kim, Min Jae Jo, Ji Hyun Lee, Jinhee Yang, R. Brian Doctor, Orson W. Moe, Jinu Lee, Eunjoon Kim and Min Goo Lee

J. Biol. Chem. 2006, 281:1461-1469.
doi: 10.1074/jbc.M509786200 originally published online November 17, 2005

THE JOURNAL OF BIOLOGICAL CHEMISTRY VOL. 281, NO. 3, pp. 1461–1469, January 20, 2006

Shank2 Associates with and Regulates Na^+/H^+ Exchanger 3*[S]

Received for publication, September 6, 2005, and in revised form, November 16, 2005 Published, JBC Papers in Press, November 17, 2005, DOI 10.1074/jbc.M509786200

WonSun Han[‡], Kyung Hwan Kim[‡], Min Jae Jo[‡], Ji Hyun Lee[‡], Jinhee Yang[§], R. Brian Doctor[¶], Orson W. Moe[‖], Jinu Lee[**], Eunjoon Kim[§], and Min Goo Lee[‡1]

*From the [‡]Department of Pharmacology, Brain Korea 21 Project for Medical Science, Institute of Gastroenterology, Yonsei University College of Medicine, Seoul 120-752, Korea, the [§]Creative Research Center for Synaptogenesis and Department of Biological Sciences, Korea Advanced Institute of Science and Technology, Guseong-dong, Daejeon 305-701, Korea, the [¶]Department of Medicine, University of Colorado Health Science Center, Denver, Colorado 80439, the [‖]Department of Internal Medicine, University of Texas Southwestern Medical Center, Dallas, Texas 75390, and the **Department of Pharmacology, Pochun CHA University College of Medicine, Sungnam 463-836, Korea*

Na^+/H^+ exchanger 3 (NHE3) plays a pivotal role in transepithelial Na^+ and HCO_3^- absorption across a wide range of epithelia in the digestive and renal-genitourinary systems. Accumulating evidence suggests that PDZ-based adaptor proteins play an important role in regulating the trafficking and activity of NHE3. A search for NHE3-binding modular proteins using yeast two-hybrid assays led us to the PDZ-based adaptor Shank2. The interaction between Shank2 and NHE3 was further confirmed by immunoprecipitation and surface plasmon resonance studies. When expressed in PS120/NHE3 cells, Shank2 increased the membrane expression and basal activity of NHE3 and attenuated the cAMP-dependent inhibition of NHE3 activity. Furthermore, knock-down of native Shank2 expression in Caco-2 epithelial cells by RNA interference decreased NHE3 protein expression as well as activity but amplified the inhibitory effect of cAMP on NHE3. These results indicate that Shank2 is a novel NHE3 interacting protein that is involved in the fine regulation of transepithelial salt and water transport through affecting NHE3 expression and activity.

Maintenance of intracellular and systemic pH, Na^+ concentration, and fluid volume is essential for maintaining the physiological status in cells and whole organisms (1, 2). First demonstrated almost 30 years ago (3), members of the mammalian Na^+/H^+ exchanger (NHE)[2] family participate in the regulation of these parameters at both cellular and systemic levels. To date, nine NHE family members have been identified in mammalian cells with unique tissue distribution and functional properties (2). As a better characterized isoform, NHE3 is primarily found in the apical membrane of epithelial cells of the renal and gastrointestinal tracts, where it mediates transepithelial absorption of Na^+ and HCO_3^- (2, 4). Lack of NHE3 activity impairs acid-base balance and extracellular fluid volume homeostasis (5).

NHE3 is known to be regulated by a large variety of hormones, such as α- and β-adrenergic agonists, dopamine, parathyroid hormone, and angiotensin II via multiple signaling systems (6, 7), but the exact underlying mechanisms are still only partially understood. Nevertheless, it has been known for many years that acute regulation of NHE3 activity is linked to protein phosphorylation, as in the case of inhibition by cAMP-dependent protein kinase A (PKA) (7, 8). Subsequently, it has been demonstrated that adaptor proteins with PDZ (PSD-95/discs large/ZO-1) domains play an important role in the cAMP-dependent inhibition of NHE3 in a number of systems (7, 9, 10). For example, EBP50 (also known as NHERF1) and E3KARP (also known as NHERF2, SIP-1, or TKA-1) were found to be necessary modular proteins that participated in the cAMP-dependent PKA phosphorylation of NHE3 by forming a multiprotein signaling complex (11, 12).

In recent years, there has been a growing interest in PDZ domains and modular proteins having PDZ domains. Best studied in the post-synaptic density (PSD) region of neurons, PDZ domain proteins have emerged as a large and important group of proteins that sequester functionally related groups of receptor, regulatory, and effector proteins into integrated molecular complexes (13–15). Epithelial cells also utilize specific PDZ proteins to direct the polarized activities in their apical and basolateral membranes. Recently, the PDZ-based scaffold protein Shank2 has been shown to be distributed to the apical pole of pancreatic, colonic, hepatic, and renal epithelia and modulate the activity of specific transport proteins, including cystic fibrosis transmembrane conductance regulator and the type IIa sodium phosphate cotransporter (16–18). Shank proteins are a family of newly identified scaffold proteins known to serve as a central coordinator of membrane protein complexes in PSD (13, 14). Currently there are three known members of the Shank family: Shank1, Shank2, and Shank3. Among them, we found that the PDZ domain of Shank2 binds to the carboxyl terminus of NHE3 in an exploratory yeast two-hybrid assay. The present study aimed to identify and characterize the biochemical nature and physiological significance of the association between Shank2 and NHE3 using integrative molecular physiological approaches.

Upon Shank2 expression, the membrane expression and basal activity of NHE3 were increased but the cAMP-dependent inhibition of NHE3 activity was attenuated in the PS120/NHE3 cells. Furthermore, knock-down of native Shank2 expression by RNA interference evoked a remarkable decrease in endogenous NHE3 activity in Caco-2 colonic epithelial cells. Thus, Shank2 appears to be a critical regulatory protein that affects NHE3 expression and activity.

EXPERIMENTAL PROCEDURES

Cell Culture and Transfection—NHE-deficient hamster fibroblast cells (PS120) were maintained in Dulbecco's modified Eagle's medi-

* This work was supported by the Korea Research Foundation, Ministry of Education & Human Resources Development (Grant R02-2004-000-10091-0) and the Korea Health 21 R&D Project, Ministry of Health & Welfare, Korea (Grant 03-PJ10-PG13-GD01-0002). The costs of publication of this article were defrayed in part by the payment of page charges. This article must therefore be hereby marked "*advertisement*" in accordance with 18 U.S.C. Section 1734 solely to indicate this fact.

The nucleotide sequence(s) reported in this paper has been submitted to the GenBank™/EBI Data Bank with accession number(s) DQ152234.

[S] The on-line version of this article (available at http://www.jbc.org) contains supplemental table S1.

[1] To whom correspondence should be addressed. Tel.: 82-2-2228-1737; Fax: 82-2-313-1894; E-mail: mlee@yumc.yonsei.ac.kr.

[2] The abbreviations used are: NHE, Na^+/H^+ exchanger; PKA, cAMP-dependent protein kinase; PKA-anchoring protein, cAMP-dependent protein kinase anchoring protein; EIPA, 5-(*N*-ethyl-*N*-isopropyl) amiloride; PDZ, PSD-95/discs large/ZO-1; PCD, post-confluent day; PSD, post-synaptic density; siRNA, small interfering RNA; CMV, cytomegalovirus; aa, amino acid(s); EST, express sequence tag; KCLB, Korea Cell Line Bank.

um-HG (Invitrogen) supplemented with 10% fetal bovine serum and penicillin (50 IU/ml)/streptomycin (50 μg/ml). The pCMV-rNHE3 construct was a generous gift from Dr. K. Park at Juseong University, Korea (19) and was stably transfected into a PS120 cell line using Lipofectamine Plus Reagent (Invitrogen). NHE3 stable transfectants (PS120/NHE3) were selected by resistance to antibiotic Geneticin (G418 Invitrogen) and by an H^+-killing method (20). The constructs of pcDNA3.1-rShank2/CortBP1 (21) and pcDNA3.1-rShank2E (18) were transiently transfected into PS120/NHE3 cells with or without pcDNA3.1-EBP50/NHERF1 (9) using Lipofectamine Plus Reagent. Caco-2 cells (human colon adenocarcinoma cells) were grown at 37 °C in a 5% CO_2-95% air environment. The culture medium consisted of Dulbecco's modified Eagle's medium-HG, 10% fetal bovine serum, 50 IU/ml penicillin, and 50 μg/ml streptomycin. Cells reached confluence after 5–7 days in culture. They were used for experiments at least 7 days after confluence, and the incubation medium was freshly changed on alternate days.

Yeast Two-hybrid Analysis—The yeast two-hybrid assay was performed as described earlier (22). The L40 yeast strain harboring the reporter genes *HIS3* and *LacZ*, under control of the upstream LexA DNA-binding domain was used in the assay. To semi-quantify the interaction, *HIS3* activity was determined by the percentage of yeast colonies growing on histidine-lacking medium. cDNA sequences containing the carboxyl-terminal 32 aa of rNHE3 (aa 800–831: PFRLSNKSVDSFLQADGPEEQLQPASPESTHM) were amplified by PCR and subcloned in-frame into pBHA construct (a bait vector containing the *LexA* DNA-binding domain). The pGAD10 (a prey vector, Clontech) constructs containing the PDZ domains of SAP97, PSD-95, S-SCAM, and Shank2 were previously described (16).

Surface Plasmon Resonance Measurements and Kinetic Analysis of Sensorgrams—Regions corresponding to residues of Shank2 PDZ (1–142) and of EBP50/NHERF1 PDZ1–2 (1–296) were PCR-amplified and cloned into pRSET-A vector (Invitrogen) to create His-tagged constructs. Amino-terminal 32-aa residues of rNHE3 (NM_012654) were PCR-amplified and cloned into pGEX-4T-1 vector (Amersham Biosciences) to create glutathione *S*-transferase fusion constructs. All constructs were confirmed by sequence analysis. All fusion proteins were expressed in *Escherichia coli* BL21(DE3) cells and purified on nickel-nitrilotriacetic acid resin (Qiagen, Venlo, Netherlands) and glutathione-Sepharose 4B (Amersham Biosciences), as appropriate. The purified proteins were quantified with Bio-Rad protein assay reagent, and their purity was assessed as >90% by Coomassie Blue staining of SDS-PAGE gels.

A surface plasmon resonance system equipped with nitrilotriacetic acid chip (BIAcore 3000, Biacore AB, Uppsala, Sweden) was used for the capturing of His-tagged PDZ fusion proteins. Analytes (glutathione *S*-transferase-tagged C-terminal 32 aa of rNHE3) at various concentrations in HEPES-buffered saline-EP (0.01 M Hepes, 0.15 M NaCl, 50 μM EDTA, 0.005% Tween 20, pH 7.4) were perfused at a flow rate of 30 μl/min. The sensor chip was regenerated between each analysis using successive injections of solutions containing 0.15 M NaCl and 0.35 M EDTA. At least two replicate experiments were performed for each fusion protein. Response curves were generated by subtraction of the background signal generated simultaneously by the control flow cell. The background-subtracted curves were prepared for fitting by subtracting the signal generated by buffer alone on experimental flow cells. Sensorgram curves were evaluated by the BIAEVALUATION 3.0 software (Biacore AB), which uses numerical integration algorithms.

Immunoblotting and Immunoprecipitation—PS120 or Caco-2 cell lysates (~2 mg of protein) were mixed with the appropriate antibodies and incubated overnight at 4 °C in lysis buffer. Immune complexes were collected by binding to protein G/A-Sepharose and washed four times with lysis buffer prior to electrophoresis. The immunoprecipitates or lysates (50 μg of protein) were suspended in SDS sample buffer and separated by SDS-polyacrylamide gel electrophoresis. The separated proteins were transferred to nitrocellulose membranes, and the membranes were blocked by a 1-h incubation at room temperature in 5% nonfat dry milk in a solution containing 20 mM Tris-HCl, pH 7.5, 150 mM NaCl, and 0.05% Tween 20. The membranes were then incubated with the appropriate primary and secondary antibodies, and protein bands were detected with enhanced chemiluminescence solutions. Rabbit polyclonal 1568 antisera against NHE3 (23) and 1136 antisera against Shank2 (20) were described previously. Mouse monoclonal antibody against the carboxyl terminus of human β-actin was purchased from Santa Cruz Biotechnology (Santa Cruz, CA). Rabbit polyclonal antibodies against NHE1 and NHE2 were from Dr. S. Grinstein, Hospital for Sick Children, Toronto, Canada and Dr. E. Chang, University of Chicago, IL, respectively, and the specificity of each antibody was verified in previous reports (24–26).

Cell-surface Biotinylation Assay—PS120/NHE3 and PS120/NHE3/rShank2 cells were grown to 70–80% confluence in 6-cm Petri dishes. The cells were then placed at 4 °C and then washed twice in phosphate-buffered saline and once in borate buffer (in mM: 154 NaCl, 10 boric acid, 7.2 KCl, 1.8 $CaCl_2$, pH 9.0). The plasma membrane proteins were then biotinylated by gently shaking the cells in a borate buffer containing sulfo-NHS-SS-biotin (Pierce) for 30 min. After biotinylation, the cells were washed extensively with quenching buffer to remove excess biotin and then washed twice with phosphate-buffered saline. The cells were then lysed, and NeutrAvidin solution (UltraLink Immobilized NeutrAvidin Beads 10%, Pierce) was added to the supernatant and the mixture was incubated at 4 °C overnight. Avidin-bound complexes were pelleted (13,000 rpm) and washed three times. Biotinylated proteins were eluted in Laemmli buffer, resolved by SDS-PAGE, electrotransferred, and immunoblotted with NHE3 antibody.

Genome Screening, Reverse Transcription-PCR, and cDNA Sequencing—To identify the epithelial splice variant of human Shank2 (hShank2E), the 400,000 bp upstream of the start codon of hShank2 (a homologous protein of rCortBP1, accession number NM_012309) on human chromosome 11 was analyzed using the rat Shank2E sequence as a reference sequence (rShank2E, accession number AY298755). Putative exons were determined by the New GENSCAN web server at the Massachusetts Institute of Technology. A list of candidate exons were chosen with > 5 scoring, translated into protein sequence, and aligned with that of rShank2E. During this process, non-homologous exons were excluded. A human EST AK096045 was also used for the analysis of the hShank2E sequence. To confirm the hShank2E sequence, PCR primers specific to hShank2E, especially to the ankyrin repeats domain were designed and cDNA products were sequenced using an ABI-Prism sequencer. Reverse transcription-PCR using a primer set from exons 1 and 17 produced a 2,122-bp band, and the whole DNA sequence of this product was submitted to the GenBank™ data base with accession number DQ152234 (see Fig. 5). hShank2E cDNA sequence from exons 1–8 was identical to that of a partial EST clone isolated from human kidney (AK096045) except exon 2, where an internal alternative splicing is evident in the EST clone. We could not find sequences corresponding to exon 8 on the human genome contig of chromosome 11 (NT_033927), although our sequence perfectly matched with that of the EST (AK096045) clone. It could be either from short repeated exons in the region or erroneous information in the genome contig. In addition, a PCR primer set that can specifically detect hShank2/CortBP1 was

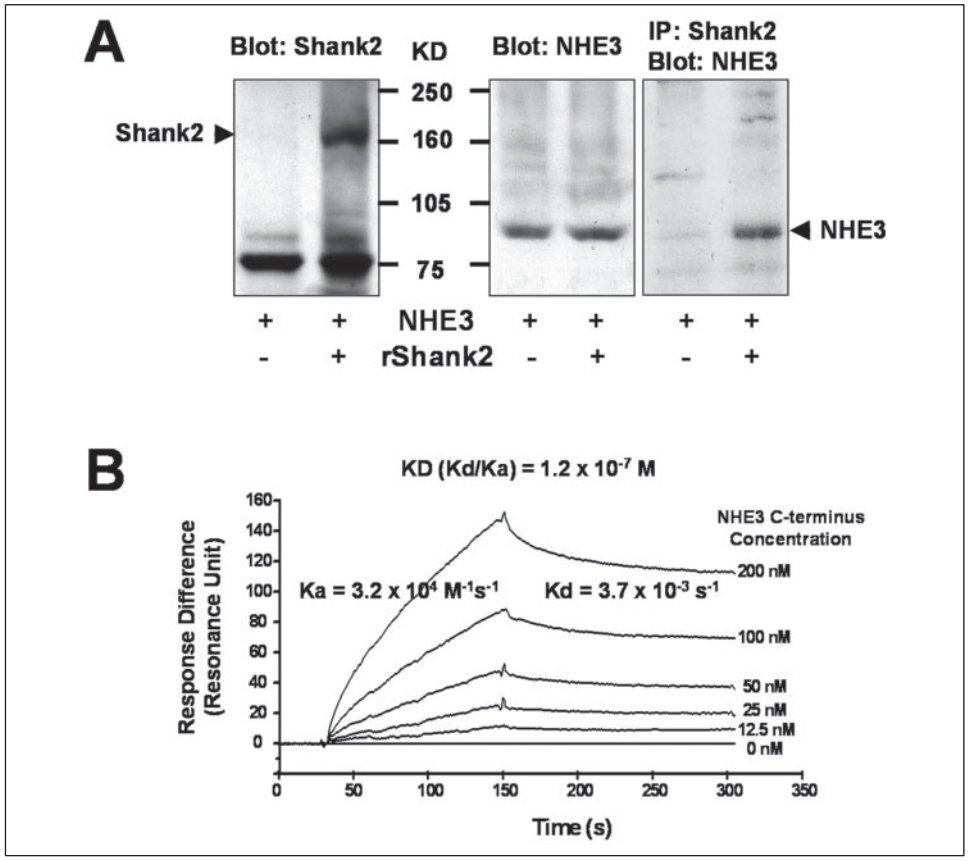

FIGURE 1. **Protein-protein interaction between Shank2 and NHE3.** *A*, immunoprecipitation. Whole cell lysates of PS120/NHE3 cells transiently transfected with pcDNA3.1-rShank2/CortBP1 or mock plasmids were immunoprecipitated with Shank2 antibody and characterized by immunoblotting with NHE3 antibody. *B*, surface plasmon resonance (SPR) assay. His-tagged Shank2 PDZ domain was captured with an nitrilotriacetic acid chip, and various concentrations of peptides containing the C-terminal 32 aa of NHE3 were perfused at a flow rate of 30 μl/min. Association and dissociation constants shown are an average of two separate experiments.

designed to confirm the presence of this splicing variant in Caco-2 epithelial cells. The primer sequences were as follows: 1) hShank2E, sense (exon 1, 5′-ATGCCGCGCAGCCCAACATC-3′); 2) hShank2/CortBP1, sense (exon 15a, 5′-CGCTGTCCCCGGAATTCTCTCT-3′); and 3) hShank2 common, antisense (exon 17, 5′-CCTGCCGGATCATGTTCACCAC-3′). The sizes of the hShank2E and hShank2/CortBP1 PCR products were 2,122 and 295 bp, respectively (see Fig. 5*C*). The control β-actin primer sequences were as follows: hβ-actin, sense (5′-TGTGATGGTGGGAATGGGTCAG-3′) and antisense (5′-TTTGATGTCACGCACGATTTCC-3′); size of PCR product, 510 bp.

RNA Interference—To knock down Shank2 expression in Caco-2 epithelial cells, 25-bp double-stranded RNA oligonucleotides, specific for Shank2, were synthesized (Invitrogen) and transfected into cells using Lipofectamine 2000 (Invitrogen). The target small interfering RNA (siRNA) sequence was as follows: 5′-GGAATTCTCTCTACAGTGACTGCAT-3′. Four days after transfection, cells were used for NHE measurements or harvested in lysis buffer for immunoblotting.

Measurement of Na^+/H^+ Exchange Activity—Na^+/H^+ exchange activity was measured using a standard protocol with some modifications (9). Briefly, cells grown on glass coverslips were loaded with a pH-sensitive fluorescent dye 2′,7′-bis-(2-carboxyethyl)-5-(and-6)-carboxyfluorescein acetoxymethyl ester and intracellular pH (pH_i) changes were measured. When Shank2 constructs were transiently expressed (Figs. 2 and 3), a green fluorescent protein-expressing plasmid (Invitrogen) was co-transfected and pH_i measurements were performed with cells expressing high levels of green fluorescent protein as previously reported (27). The cells were acidified by an NH_4^+ (20 mM) pulse and subsequent perfusion with an Na^+-free solution. The maximal Na^+-dependent pH_i recovery was measured in cells acidified to a pH of 6.4–6.5, with or without 5 μM forskolin/100 μM isobutylmethylxanthine treatment. The standard perfusion solution contained (mM): 140 NaCl, 5 KCl, 1 $MgCl_2$, 1 $CaCl_2$, 10 glucose, and 10 Hepes (pH 7.4 with NaOH). Na^+-free solutions were prepared by replacing Na^+ with *N*-methyl-D-glucamine$^+$. The osmolarity of all solutions was adjusted to 310 mM with the major salt. Buffer capacity was calculated by measuring pH_i in response to 5–20 mM NH_4Cl pulses. In each experiment, the intrinsic buffer capacity (β_i) showed a negative linear relationship with pH_i between 6.4 and 7.3. The β_i of PS120/NHE3 cells (34.1 ± 3.9 mM NH_4^+/pH unit at $pH_i = 7.0$) was lower than that of Caco-2 cells (44.4 ± 3.5). However, neither forskolin treatment nor any gene modulation significantly changed β_i. Therefore, all of the results of NHE activity are expressed as ΔpH/min, and this value was directly analyzed without compensating for β_i. The results are presented as means ± S.E., and, when appropriate, statistical analysis was performed using Student's *t* test or analysis of variance. A *p* value less than 0.05 was considered statistically significant.

RESULTS

Specific Binding between Shank2 PDZ and the Carboxyl Terminus of NHE3—It has been repeatedly reported that the carboxyl terminus of NHE3 plays an important role in both surface expression and regulation of the activity of NHE3 through interactions with the PDZ-domain of NHERF family proteins (7, 10). In a previous study (16) and in preliminary experiments for the present study, we observed that pancreatic and colonic epithelia express several PDZ-based adaptor proteins in addition to NHERF family proteins using reverse transcription-PCR. These include SAP97, PSD-95, S-SCAM, and Shank2 proteins. Therefore, we hypothesized that the carboxyl terminus of NHE3 may associate with other PDZ-based adaptors in epithelia. To explore the possible protein-protein interactions between the carboxyl terminus of NHE3 and the PDZ domains of these adaptor proteins, we performed a semi-quantitative yeast two-hybrid assay. As presented in supplementary Table S1,

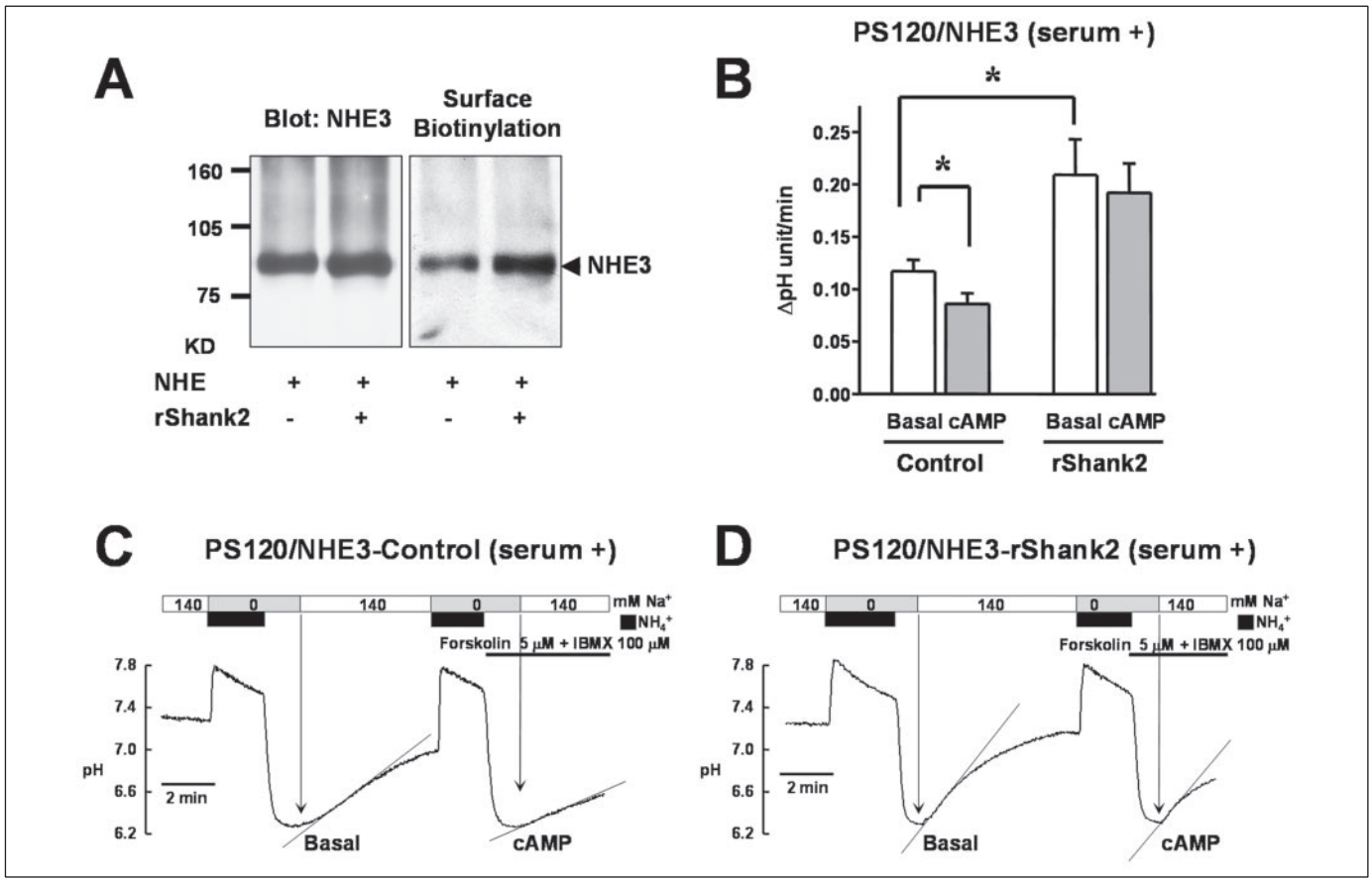

FIGURE 2. **Effects of Shank2 expression on NHE3 in PS120/NHE3 cells.** *A*, whole cell lysates and surface biotinylated proteins from PS120/NHE3 cells transiently transfected with pcDNA3.1-rShank2/CortBP1 or mock plasmids were immunoblotted with NHE3 antibody. Three separate experiments showed similar results. *B–D*, basal and cAMP-stimulated (forskolin (5 μM) plus isobutylmethylxanthine (100 μM)) NHE activities were measured in PS120/NHE3 cells kept in serum-supplemented conditions. Representative traces from cells transfected with mock plasmids and pcDNA3.1-rShank2/CortBP1 are shown in *C* and *D*, respectively, and a summary of multiple experiments ($n = 7$ for each) is depicted in *panel B*. *, $p < 0.05$.

the PDZ domain of Shank2 showed a potent induction of both *HIS3* and β-galactosidase reporter genes in yeast, indicating a direct protein-protein interaction between the carboxyl terminus of NHE3 and the PDZ-domain of Shank2.

To verify the interaction between NHE3 and Shank2 in mammalian cells, PS120 cells stably expressing NHE3 (PS120/NHE3) were transiently transfected with pcDNA3.1-rShank2/CortBP1 or with mock plasmids, and immunoprecipitation experiments were performed. As shown in Fig. 1*A*, transfection of pcDNA3.1-rShank2 induced the expression of Shank2 protein with a molecular mass of about 165 kDa (*arrowhead*). Notably, a prominent NHE3 signal was always detected in the Shank2 immunocomplexes precipitated from rShank2-transfected cells in a total of three experiments.

The binding kinetics between the Shank2 PDZ domain and the carboxyl terminus of NHE3 were analyzed by surface plasmon resonance experiments. As depicted in Fig. 1*B*, Shank2 PDZ domain captured in nitrilotriacetic acid chips specifically binds to the carboxyl terminal 32 aa of NHE3, and its overall dissociation constant at equilibrium status (K_D) was calculated as 1.2×10^{-7} M, which was within a range similar to that of interaction between the carboxyl terminus of NHE3 and EBP50/NHERF1 (1.5×10^{-7} M, figure not shown).

Functional Interaction between Shank2 and NHE3 in PS120 Cells—To investigate the functional significance of Shank2 binding on NHE3 activity, the impact of Shank2 on the surface distribution and activity of NHE3 was measured. In PS120 cells that stably express NHE3, the total amount of NHE3 protein and surface-expressed proteins were compared by using immunoblotting of total cell lysates and surface biotinylated proteins, respectively, in cells transfected with pcDNA3.1-rShank2 or with mock plasmids (Fig. 2*A*). The total amount of NHE3 protein was not different in the two groups. In contrast, cell-surface expression of NHE3 was increased 2.2 ± 0.4 times in cells transiently expressing Shank2.

NHE3 activity is primarily regulated by the surface expression of NHE3 molecules. The above results imply that by modulating the surface distribution of NHE3, Shank2 might regulate the activity of NHE3 (2, 28). To test this directly, NHE activity in PS120/NHE3 cells was measured in cells concurrently expressing Shank2. NHE activity was measured as the Na^+-dependent increase in pH_i after intracellular acidification induced by an NH_4^+ pulse as detailed under "Experimental Procedures." Most studies measuring NHE3 kinetics in PS120 cells have been done under serum-deprived conditions, because serum deprivation for 18 h increases NHE3 activity and expression (9). However, the initial set of NHE3 measurements in the present study was done under serum-supplemented conditions, because the induction of NHE3 expression by serum deprivation would deter the innate regulation of NHE3 in PS120 cells and also because immunoblotting and surface biotinylation results shown in Fig. 2*A* were performed under serum-supplemented conditions. In fact, we observed that serum deprivation blunted the Shank2-induced increase in NHE3 surface expression (data not shown). Traces of NHE activity measurements are shown in Fig. 2 (*C* and *D*), and a summary of results is illustrated in Fig. 2*B*. Notably, the basal NHE activity was increased 1.8 ± 0.3-fold upon Shank2 expres-

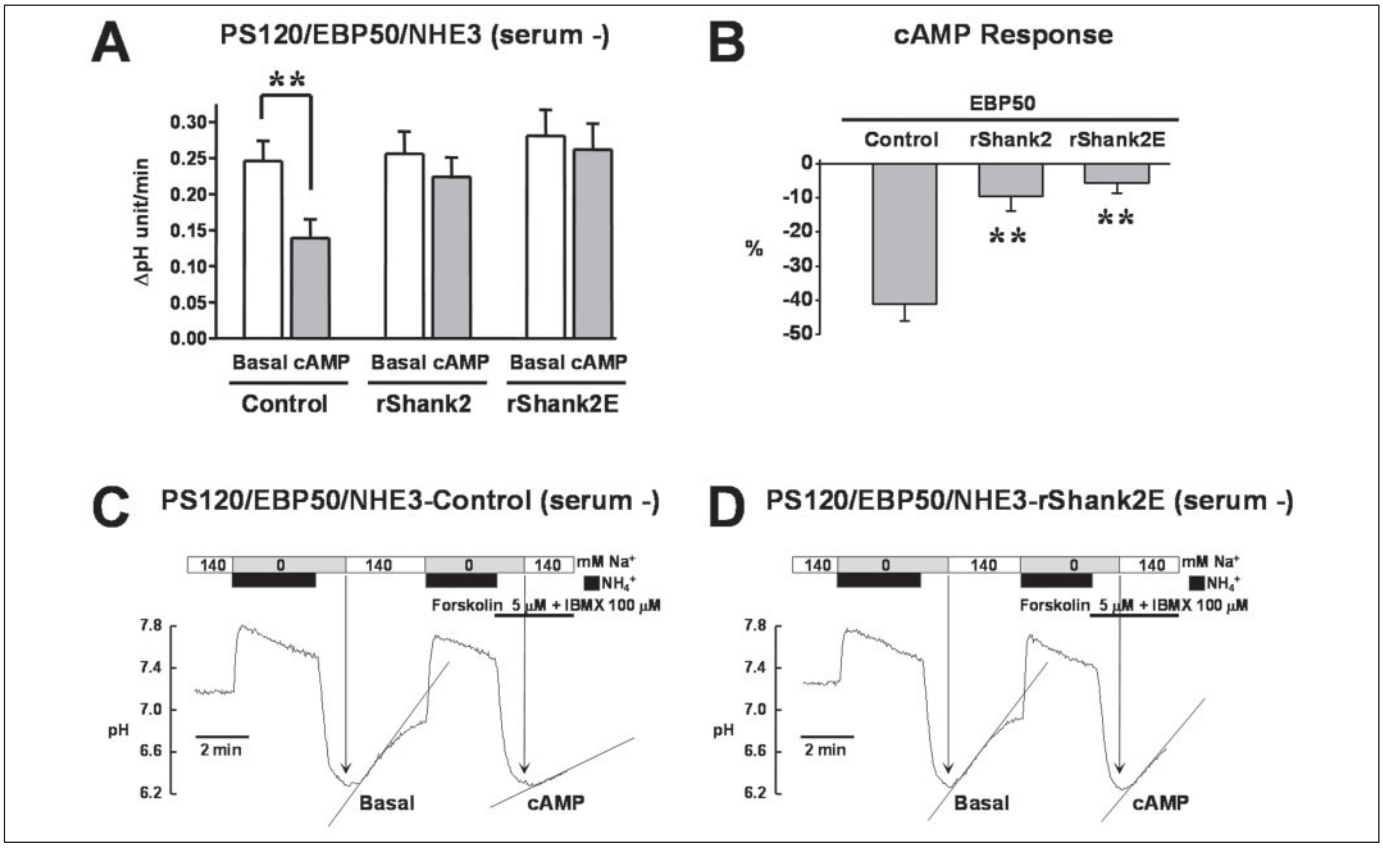

FIGURE 3. **Effects of Shank2 on cAMP-dependent inhibition of NHE3.** Basal and cAMP-stimulated NHE activities were measured in PS120/NHE3 cells transfected with mock plasmids, pcDNA3.1-rShank2/CortBP1, or pcDNA3.1-rShank2E. To observe a strong basal activity and a large cAMP-induced inhibition, PS120/NHE3 cells were deprived of serum for 18 h and co-transfected with EBP50/NHERF1-expressing plasmids. Representative traces from cells transfected with mock plasmids and pcDNA3.1-rShank2E are shown in *C* and *D*, respectively. Summaries of NHE activity and percentile inhibition of NHE activity by cAMP treatment (Control $n = 7$, rShank2 $n = 8$, rShank2E $n = 9$) are shown in *A* and *B*, respectively. **, $p < 0.01$.

sion, which correlates with the results of NHE3 surface biotinylation. In a previous study, we found that cAMP-dependent inhibitory regulation of NHE3 was partially retained in PS120 cells, in particular, when the cells were kept in serum-supplemented conditions due to a minimal endogenous expression of EBP50/NHERF1 (9). Therefore, NHE activity was measured under basal and cAMP-stimulated conditions. When the cells were treated with the cAMP mixture (forskolin 5 μM plus 3-isobutyl-1-methylxanthine, 100 μM), NHE activity was decreased by 21 $\pm$ 5% in control PS120/NHE3 cells and showed a statistically significant difference from the basal activity ($p = 0.011$). Interestingly, Shank2 expression attenuated the cAMP-dependent inhibition. In PS120/NHE3 cells transiently transfected with Shank2, cAMP treatment inhibited NHE activity by only 7 $\pm$ 5%, a significantly smaller reduction in NHE activity compared with control PS120/NHE3 cells ($p = 0.451$).

cAMP-mediated regulation of NHE3 within renal and intestinal epithelia is important in maintaining systemic pH and electrolyte homeostasis (2, 7). Therefore, the effects of Shank2 on cAMP-dependent inhibition of NHE3 were further examined using a more sophisticated system (Fig. 3). In this set of experiments, EBP50/NHERF1 was co-expressed to maximally enhance the cAMP-mediated inhibition, and serum was omitted from culture media for 18 h to increase basal NHE3 activity as well as to minimize the Shank2-induced increase in basal activity. In addition, experiments studying the effects of Shank2E, a splicing variant of Shank2 that is principally found in epithelial tissues (17), were also included. cAMP treatment decreased NHE3 activity by 41 $\pm$ 5% in EBP50/NHERF1-expressing cells. When Shank2 or Shank2E was co-expressed, cAMP-dependent inhibition of NHE3 activity was remarkably attenuated (Fig. 3*B*). Although Shank2E has additional protein domains besides those present in Shank2 (see Fig. 5*A*), there was no significant difference in their ability to attenuate cAMP-dependent inhibition of NHE3 in PS120 cells.

Expression of Shank2 and NHE3 in Caco-2 Colonic Epithelial Cells—To identify the physiological significance of Shank2-NHE3 interaction, it is necessary to examine the effects of endogenous Shank2 on native NHE3 activity in epithelial cells. Caco-2 cells originated from human colonic epithelia are known to express NHE3, and the benefits of using Caco-2 cell clones as an *in vitro* model for studies on physiology of NHE3 have been reported (29). We screened Caco-2 cells from two different sources, the American Type Culture Collection (ATCC, HTB-37) and the Korea Cell Line Bank (KCLB, 30037). Because the cells from KCLB showed greater Shank2 expression (see below), we used this batch of cells for further experiments. In pilot studies, NHE3 expression was not detected in Caco-2 cells harvested at post-confluent day (PCD) 0 and 2 (Fig. 4). In contrast, PCD 5 cells expressed NHE3 and NHE3 protein level was the greatest at PCD 7. Consistent with protein expression levels, NHE3 activity was detected in cells at PCD 7 but not PCD 0 (Fig. 4, *B* and *C*). This gradual development of the NHE3 expression is similar to other proteins expressed at the brush border of Caco-2 cells such as sucrase-isomaltase, lactase, and alkaline phosphatase (30). Based on these results, all the subsequent Caco-2 experiments were done on or after PCD 7.

Expression of Shank2 was also identified in Caco-2 cells. It has been demonstrated that rat epithelial cells expressed rShank2E, a different spliceoform of rShank2/CortBP1 and ProSAP1A that had been identi-

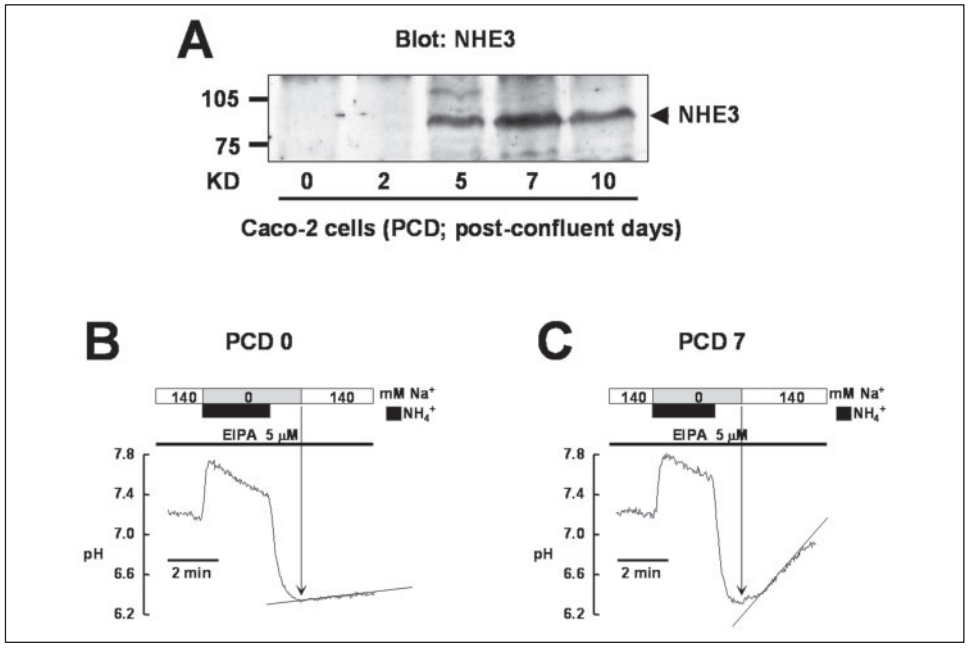

FIGURE 4. **NHE3 expression in Caco-2 cells.** *A*, NHE3 expression was verified in Caco-2 cells (KCLB, 30037) collected on post-confluent days (*PCD*) 0, 2, 5, 7, and 10 by immunoblotting with NHE3 antibody. *B* and *C*, NHE3 activities were measured in Caco-2 cells after treatment with EIPA 5 μM to inhibit NHE1 and NHE2 isoforms. Cells on PCD 7 showed a 5 μM EIPA-resistant NHE activity (*C*), while cells on PCD 0 showed no identifiable 5 μM EIPA-resistant NHE activities (*B*). Cells using a different batch of Caco-2 cells (ATCC, HTB-37) showed similar results.

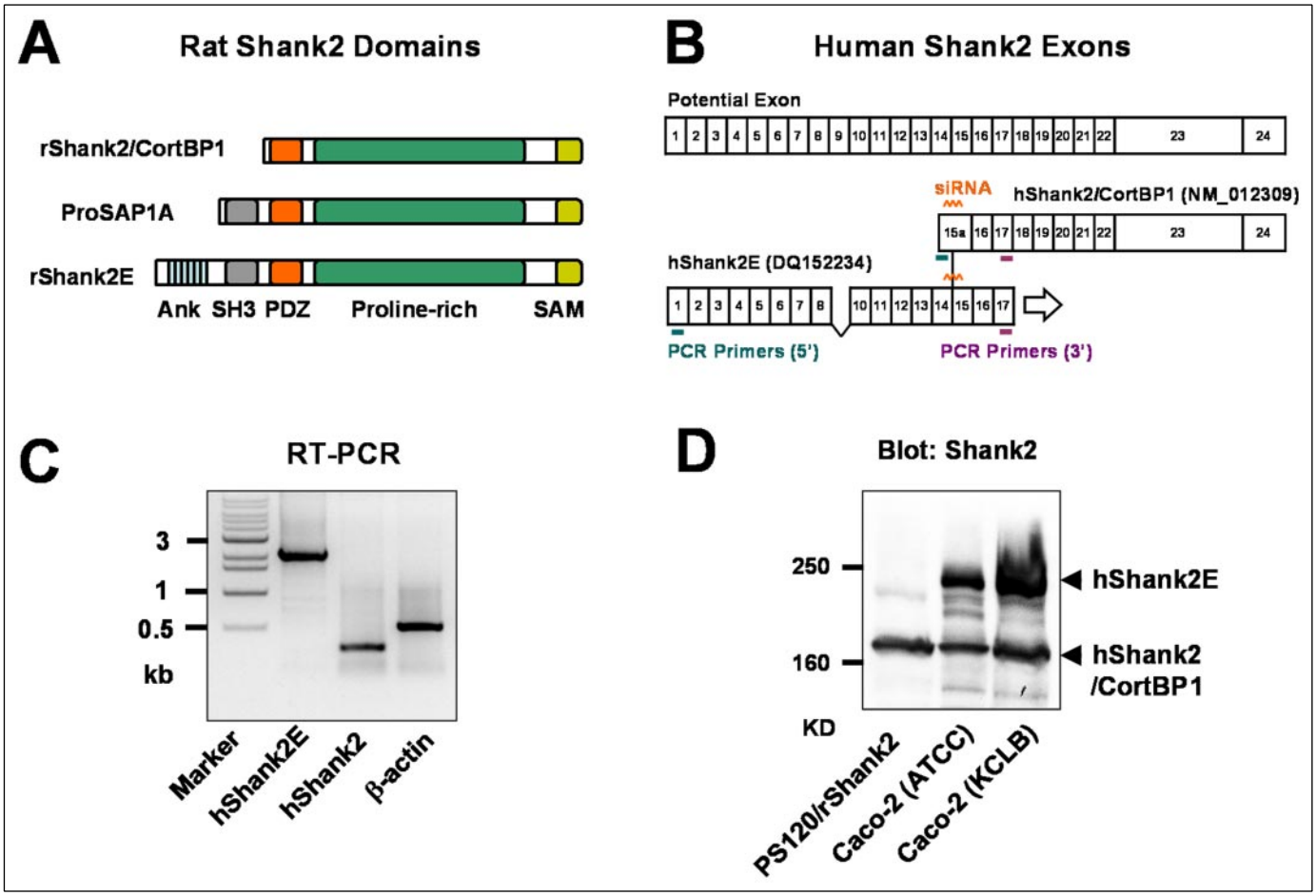

FIGURE 5. **Expression of Shank2 proteins in Caco-2 cells.** *A*, domain compositions of rat Shank2 splicing variants. *B*, exon structures of human Shank2 splicing variants isolated in Caco-2 cells. Existence of exon 9 was observed in a partial EST clone (AK096045). *C*, PCR reactions on cDNA prepared from Caco-2 cells revealed that Caco-2 cells express mRNAs of both hShank2E and hShank2/CortBP1 isoforms. Primer locations for each Shank2 isoform are presented in *panel B*. *D*, endogenous expression of Shank2 protein was verified in two different batches (ATCC, HTB-37; KCLB, 30037) of Caco-2 cells by blotting with Shank2 antibody. Protein sample of control lane (*left-hand lane*) was prepared from PS120/NHE3 cells transfected with rShank2/CortBP1.

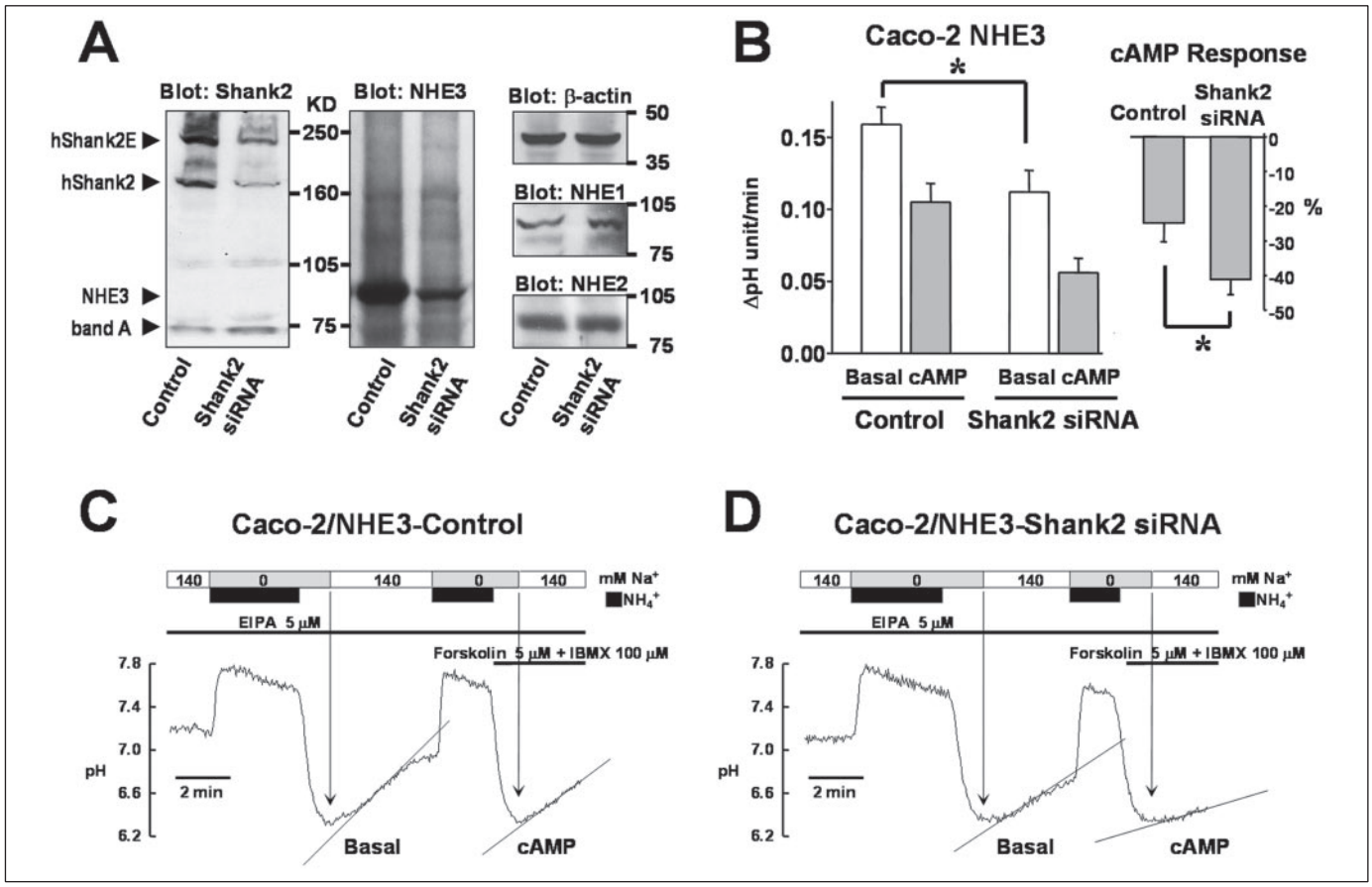

FIGURE 6. **Effect of Shank2 loss on NHE3 in Caco-2 cells.** *A*, equal amounts (50 μg) of protein samples from Caco-2 cells (KCLB, 30037) treated with mock or Shank2 siRNA were immunoblotted against Shank2 antibody (*left panel*), NHE3 antibody (*middle panel*), and β-actin, NHE1 and NHE2 antibodies (*right panel*). *B–D*, basal and cAMP-stimulated (Forskolin (5 μM) plus isobutylmethylxanthine (100 μM)) NHE3 activities were measured in Caco-2 cells treated with mock or Shank2 siRNAs. Representative traces are shown in *C* and *D*, and summaries of multiple experiments (Control $n = 6$, Shank2 siRNA $n = 5$) are presented in *B*. *, $p < 0.05$.

fied in rat brain (17) (Fig. 5*A*). Therefore, we attempted to investigate the human homologues of these isoforms as detailed under "Experimental Procedures." PCR reactions using multiple primer sets on cDNA prepared from Caco-2 cells revealed that Caco-2 cells express at least two different isoforms, hShank2/CortBP1 and hShank2E. hShank2E was a homologue of rShank2E, and the N-terminal coding sequence of its mRNA had 13 additional exons not present in the hShank2 mRNA (accession number DQ152234, Fig. 5*B*). Reverse transcription-PCR using a primer set from exons 1 and 17 produced a 2122-bp band specific to hShank2E (Fig. 5, *B* and *C*). The open reading frame of hShank2/CortBP1 starts 89 bp upstream of exon 15 (exon 15a), and its sequence was identical to that of the previously identified hShank2 in human brain (NM_012309). Reverse transcription-PCR using a primer set from exons 15a and 17 produced an expected 295-bp band of hShank2 in Caco-2 cells (Fig. 5, *B* and *C*). Finally, expression of both hShank2E and hShank2 in Caco-2 cells was demonstrated by immunoblotting. We tested two batches of Caco-2 cells from ATCC and KCLB. Basically, they showed identical band patterns, a 165-kDa band corresponding to hShank2/CortBP1 and a 240-kDa band corresponding to hShank2E, although the batch from KCLB expressed slightly more of both Shank2 proteins (Fig. 5*D*). When analyzing band intensities, it was found that the amount of Shank2E protein was 1.8 $\pm$ 0.2-fold higher than that of Shank2/CortBP1 in Caco-2 cells.

Effect of Shank2 Knock-down on NHE3 in Caco-2 Epithelial Cells—To determine whether Shank2 has any physiologically relevant effects on NHE3, RNA interference was used to knock down Shank2 expression in Caco-2 cells. We designed several sets of siRNAs, and one of these, which acted on exon 15a, showed a good effect in inhibiting Shank2 expression. This siRNA on exon 15a was designed to break down RNAs of hShank2. However, 12 nucleotides at its 3′-end (sense strand) were perfectly matched with the beginning region of exon 15 of Shank2E and also inhibited hShank2E expression. This could be due to an inhibition of translation observed in small RNAs that matched to the 3′ region of target mRNA (5′ region of the antisense strand of siRNA) (31). Transfection of siRNA in Caco-2 cells decreased protein expression of hShank2 and hShank2E by 89 $\pm$ 4% and 76 $\pm$ 8%, respectively (Fig. 6*A*, *left panel*). Importantly, knock-down of Shank2 was paralleled by a loss of NHE3 protein (52 $\pm$ 8%) compared with control cells (Fig. 6*A*, *middle panel*). Treatment of siRNA has been noted for the knock-down of non-related genes. However, the persistent expression of a nonspecific band detected by anti-Shank2 1136 antibody when treated with Shank2 siRNA (Fig. 6*A*, *left panel*, *band A*) suggests that the siRNA used is specific for Shank2 RNAs. In addition, the expression levels of β-actin, NHE1, and NHE2 were not affected by Shank2 siRNA treatment (Fig. 6*A*, *right panel*).

Lastly, the effects of Shank2 loss on NHE3 activity were investigated in Caco-2 cells. NHE3 activity was measured using protocols similar to those used in PS120/NHE3 cells, except that 5 μM 5-(*N*-ethyl-*N*-isopropyl) amiloride (EIPA) was added to inhibit NHE1 and NHE2 that expressed in Caco-2 cells (32). Individual traces of NHE activity measurement are shown in Fig. 6 (*C* and *D*), and summaries of the results are illustrated in Fig. 6*B*. In agreement with the findings from immunoblot-

ting, basal NHE3 activity was reduced upon Shank2 loss. Moreover, the cAMP response of inhibiting NHE3 was increased in the Shank2 siRNA-treated cells, and this result exactly matched the cAMP response observed in the heterologous expression system of PS120/NHE3 cells (Fig. 3). Therefore, it was concluded that Shank2 affects cAMP signaling on NHE3 activity as well as NHE3 expression in Caco-2 epithelia.

DISCUSSION

Sequestering specific membrane proteins into apical and basolateral compartments is critical for development, maintenance, and regulated function of polarized epithelia. PDZ-based molecular adaptors have emerged as key organizers of epithelial microdomain structures that govern epithelial polarity and vectorial transport (33, 34). In the present study, we report a novel protein-protein interaction between the PDZ-based scaffold Shank2 and an epithelial transporter NHE3, which affects membrane expression and cAMP-dependent regulation of the transporter.

NHE3 is one of five plasma membrane Na^+/H^+ exchangers and is encoded by SLC9A3 in humans. It is expressed on the apical membranes of renal proximal tubule and intestinal epithelial cells. Lack of the NHE3 activity impairs acid-base balance and systemic fluid volume homeostasis (5). Many hormones, neurotransmitters, and the associated signaling systems such as cAMP, cGMP, and elevated intracellular calcium have been identified as regulators of NHE3 in various tissues and cell lines. One well studied system is the cAMP-PKA-mediated pathway (2, 7). Down-regulation of NHE3 activity by cAMP-PKA pathways involves phosphorylation of carboxyl-terminal serine residues of NHE3 *in vitro* and *in vivo* (8), and this inhibition only occurs in the presence of the PDZ-based modular adaptors, NHERF1/EBP50 or NHERF2/E3KARP, which link NHE3 to Ezrin, a low affinity PKA-anchoring protein (10). It has been shown that cAMP-PKA pathways decrease both the membrane expression of NHE3 molecules and the turnover rate of the transporter, although there have been considerable degrees of heterogeneity among the stimulating agonists and the cell types (6, 35).

In line with the regulatory mechanisms of NHE3, the present study reports two remarkable findings regarding the PDZ-containing modular protein Shank2: 1) Shank2 blunted the cAMP-dependent acute inhibition of NHE3, and 2) Shank2 increased surface expression of NHE3. The cAMP-dependent acute inhibition can be due to a change in pH_i sensitivity or V_{max} of the transporter (35) or even due to an acute decrease in surface expression (6). Although the mechanisms by which cAMP signals acutely inhibit NHE3 are diverse, protein phosphorylation by PKA type II has been demonstrated to be an essential common event (6, 8, 37). Based on the data from this study, it can be speculated that Shank2 binding can blunt the effect of cAMP-PKA either by changing the phosphorylation status of NHE3 independent of the EBP50·ezrin·PKA complex or by competing with the PDZ-based scaffolds associated with PKA-anchoring protein, thus breaching the formation of protein complexes that would lead to PKA-dependent phosphorylation. It is interesting to note that the PDZ domains of Shank proteins have a very similar three-dimensional structure to that of the PDZ1 domain of EBP50/NHERF1 (36). In particular, they contain a negatively charged amino acid at the end of the βC strand of the PDZ domain structures (Glu^{43} in hEBP50, Asp^{634} in rShank1, and Asp^{80} in hShank2), which serves the preference for a positively charged residue at the −1 position in the carboxyl terminus of membrane transporter, such as -T***R***L in cystic fibrosis transmembrane conductance regulator and -T***H***M in NHE3 (36). Therefore, it is possible that Shank2 might compete against EBP50/NHERF1 in their PDZ-ligand binding in cells expressing both adaptor proteins. Further studies on the effects of Shank2 expression on phosphorylation of NHE3 or on the possible competition for binding between Shank2 and other epithelial PDZ-based adaptors will be needed to address these questions.

In addition to the modulation of cAMP effects, Shank2 induced an increase in surface expression of NHE3. An effective and rapid way of controlling the function of cell-surface proteins is by altering the number of available molecules at the plasma membrane. Studies on the subcellular localization of NHE3 revealed the existence of a substantial intracellular pool of transporters in vesicles as well as at the membrane surface, indicating that NHE3 traffics between the plasma membrane and recycling endosomal vesicles under basal and regulated conditions (38). There could be many explanations for the increased surface level of NHE3 by Shank2, because Shank family proteins are known to be engaged in the sorting, targeting, and organizing of target proteins (13, 15). As a master scaffold, Shank holds together the *N*-methyl-D-aspartic acid receptor, metabotropic glutamate receptor and AMPA receptor complexes and promotes synaptic accumulation of βPIX and βPIX-associated signaling molecules at the PSD of excitatory synapses (21). In addition, it was found that Shank2 interacts with Dynamin, a GTPase involved in synaptic vesicle recycling, receptor-mediated endocytosis, and other types of membrane trafficking (39). This observation further supports the possibility that Shank2 is involved in the trafficking of NHE3 and promotes stable membrane expression of the transporter.

An unexpected finding in this study was the decreased NHE3 protein level following loss of Shank2 in Caco-2 cells. It should be noted that the heterologous expression system of PS120/NHE3 cells may lack some important factors specific to epithelial cells. Thus, Caco-2 cells were used as a native epithelial cell system to investigate physiological effects of Shank2 on NHE3 activity. Caco-2 cells, which natively express both Shank2 and NHE3, are a colon cancer cell line that have been used to model a number of absorptive functions of intestinal epithelial cells (29, 30). Importantly, Shank2 expression induced an increase in the total amount of NHE3 protein in Caco-2 epithelial cells. However, in the heterologous expression system of PS120/NHE3 cells, Shank2 induced an increase only in the level of surface NHE3 protein. The most plausible explanation for this difference is that the increased membrane stability of NHE3 by Shank2 can evoke an observable increase in the total amount of NHE3 in Caco-2 cells, where NHE3 expression is controlled by an innate promoter system, but not in PS120/NHE3 cells, where a large amount of NHE3 is produced by uncontrolled CMV promoters and a larger intracellular pool of NHE3 may exist. However, an alternative possibility is that Shank2 may affect the transcription of NHE3. There have been many reports suggesting the involvement of PDZ-containing proteins in the transcriptional regulation of target proteins. For example, EBP50/NHERF1 has been reported to interact with β-catenin through its carboxyl-PDZ domain and enhance β-catenin-dependent transcription in a dose-dependent manner (40). Recent studies have also reported a transcriptional coactivator TAZ with PDZ-binding motif that has been shown to interact with E3KARP/NHERF2 and to be involved in gene regulation (41). The underlying mechanisms responsible for the decreased NHE3 proteins on Shank2 loss in Caco-2 cells are currently under investigation.

Shank/CortBP/ProSAP family of PDZ-based adaptor proteins were identified independently by several investigators and suggested to be an important organizer in the postsynaptic specialization of neuronal cells (13). In epithelial cells, Shank2 isoforms (CortBP1, ProSAP1A, and Shank2E) are highly expressed in the apical pole of epithelia (16–18). Shank proteins contain multiple protein-protein interaction sites, including ankyrin repeats, an SH3 domain, a PDZ domain, a long proline-rich domain, and a SAM domain. Shank2E has all five protein inter-

action sites, whereas Shank2/CortBP1 has only the last three. In the present study, we found that both Shank2/CortBP1 and Shank2E are co-expressed in Caco-2 epithelia at an approximate 2:1 ratio. Interestingly, functional assays found no differences in the regulation of NHE2 by Shank2/CortBP1 and Shank2E. This does not mean that the two different isoforms play the same role in epithelia. Identifying the binding partners of Shank2E-specific sites in epithelia and the differential knock-out of the splicing variants will be needed to understand the specific role of each isoform.

The physiological relevance of Shank2-NHE3 interaction can be appreciated from several points. Firstly, Shank2 up-regulates surface expression of NHE3 and the basal activity of NHE3 in epithelial cells. Considering the fact that NHE3 is a major transporter in the electroneutral uptake of NaCl in intestinal epithelia and in the reabsorption of $NaHCO_3$ and NaCl in the renal proximal tubule, maintaining basal NHE3 activity is important in fluid volume, electrolyte, and acid-base homeostasis. Secondly, the inhibition of cAMP-dependent signaling on NHE3 by Shank2 also has physiological implications. NHE3 is up- and down-regulated as part of digestion, initially being inhibited and then stimulated by various neurohormonal stimuli. In addition, the cAMP-dependent inhibition is exaggerated in diarrheal disease (10). In this regard, an interesting observation is that Shank2 inhibits the cAMP-induced activation of cystic fibrosis transmembrane conductance regulator, the major secretory transporter in the intestine and colon (16). Therefore, the same protein, Shank2, regulates both absorptive and secretory epithelial transporters in a reciprocal manner, and by using this combinatorial activity Shank2 can effectively modulate net epithelial transport.

Keeping the balance of and preventing overt cAMP signaling are necessary for normal regulation of digestive physiology and for preventing severe diarrhea. It has been recognized that NHE3 exists in large multiprotein complexes in size from 200 to 1200 kDa in intestinal tissues (42). Maintaining and regulating a dynamic balance between cAMP signal-conferring and -stopping complexes would be a critical regulatory mechanism for NHE3 activity. All of the components that we have discussed (NHE3, NHERF proteins, and Shank2 proteins) have been shown to exist in renal proximal tubule cells by independent studies (7, 18). Therefore, we expect that a similar analogy may exist in the kidney epithelia, although the present study did not explore the Shank2-NHE3 interaction in kidney cells. Our findings about the role of Shank2 in the regulation of NHE3 activity and expression shed new light on the mechanisms by which salt and water transport are regulated to maintain systemic electrolyte, acid-base, and fluid volume homeostasis.

Acknowledgments—We thank Dr. K. Park at Juseong University and Dr. S. L. Milgram at University of North Carolina for their kind gifts of pCMV-NHE3 and pcDNA3.1-EBP50 constructs. We also thank Dr. S. Muallem at University of Texas Southwestern Medical Center for helpful discussions and technical assistances.

REFERENCES

1. Wakabayashi, S., Shigekawa, M., and Pouyssegur, J. (1997) *Physiol. Rev.* **77,** 51–74
2. Zachos, N. C., Tse, M., and Donowitz, M. (2005) *Annu. Rev. Physiol.* **67,** 411–443
3. Murer, H., Hopfer, U., and Kinne, R. (1976) *Biochem. J.* **154,** 597–602
4. Lee, M. G., Ahn, W., Choi, J. Y., Luo, X., Seo, J. T., Schultheis, P. J., Shull, G. E., Kim, K. H., and Muallem, S. (2000) *J. Clin. Invest.* **105,** 1651–1658
5. Schultheis, P. J., Clarke, L. L., Meneton, P., Miller, M. L., Soleimani, M., Gawenis, L. R., Riddle, T. M., Duffy, J. J., Doetschman, T., Wang, T., Giebisch, G., Aronson, P. S., Lorenz, J. N., and Shull, G. E. (1998) *Nat. Genet.* **19,** 282–285
6. Hu, M. C., Fan, L., Crowder, L. A., Karim-Jimenez, Z., Murer, H., and Moe, O. W. (2001) *J. Biol. Chem.* **276,** 26906–26915
7. Weinman, E. J., Cunningham, R., and Shenolikar, S. (2005) *Pflugers Arch.* **450,** 137–144
8. Zhao, H., Wiederkehr, M. R., Fan, L., Collazo, R. L., Crowder, L. A., and Moe, O. W. (1999) *J. Biol. Chem.* **274,** 3978–3987
9. Ahn, W., Kim, K. H., Lee, J. A., Kim, J. Y., Choi, J. Y., Moe, O. W., Milgram, S. L., Muallem, S., and Lee, M. G. (2001) *J. Biol. Chem.* **276,** 17236–17243
10. Donowitz, M., Cha, B., Zachos, N. C., Brett, C. L., Sharma, A., Tse, C. M., and Li, X. (2005) *J. Physiol.* **567,** 3–11
11. Weinman, E. J., Steplock, D., Wang, Y., and Shenolikar, S. (1995) *J. Clin. Invest.* **95,** 2143–2149
12. Yun, C. H., Oh, S., Zizak, M., Steplock, D., Tsao, S., Tse, C. M., Weinman, E. J., and Donowitz, M. (1997) *Proc. Natl. Acad. Sci. U. S. A.* **94,** 3010–3015
13. Sheng, M., and Kim, E. (2000) *J. Cell Sci.* **113,** 1851–1856
14. Lim, S., Naisbitt, S., Yoon, J., Hwang, J. I., Suh, P. G., Sheng, M., and Kim, E. (1999) *J. Biol. Chem.* **274,** 29510–29518
15. Kim, E., and Sheng, M. (2004) *Nat. Rev. Neurosci.* **5,** 771–781
16. Kim, J. Y., Han, W., Namkung, W., Lee, J. H., Kim, K. H., Shin, H., Kim, E., and Lee, M. G. (2004) *J. Biol. Chem.* **279,** 10389–10396
17. McWilliams, R. R., Gidey, E., Fouassier, L., Weed, S. A., and Doctor, R. B. (2004) *Biochem. J.* **380,** 181–191
18. McWilliams, R. R., Breusegem, S. Y., Brodsky, K. F., Kim, E., Levi, M., and Doctor, R. B. (2005) *Am. J. Physiol.* **289,** C1042–C1051
19. Park, K., Olschowka, J. A., Richardson, L. A., Bookstein, C., Chang, E. B., and Melvin, J. E. (1999) *Am. J. Physiol.* **276,** G470–G478
20. Wakabayashi, S., Fafournoux, P., Sardet, C., and Pouyssegur, J. (1992) *Proc. Natl. Acad. Sci. U. S. A.* **89,** 2424–2428
21. Park, E., Na, M., Choi, J., Kim, S., Lee, J. R., Yoon, J., Park, D., Sheng, M., and Kim, E. (2003) *J. Biol. Chem.* **278,** 19220–19229
22. Kim, E., Niethammer, M., Rothschild, A., Jan, Y. N., and Sheng, M. (1995) *Nature* **378,** 85–88
23. Amemiya, M., Loffing, J., Lotscher, M., Kaissling, B., Alpern, R. J., and Moe, O. W. (1995) *Kidney Int.* **48,** 1206–1215
24. Lee, M. G., Schultheis, P. J., Yan, M., Shull, G. E., Bookstein, C., Chang, E., Tse, M., Donowitz, M., Park, K., and Muallem, S. (1998) *J. Physiol.* **513,** 341–357
25. Robertson, M. A., Woodside, M., Foskett, J. K., Orlowski, J., and Grinstein, S. (1997) *J. Biol. Chem.* **272,** 287–294
26. Bookstein, C., Xie, Y., Rabenau, K., Musch, M. W., McSwine, R. L., Rao, M. C., and Chang, E. B. (1997) *Am. J. Physiol.* **273,** C1496–C1505
27. Lee, M. G., Wigley, W. C., Zeng, W., Noel, L. E., Marino, C. R., Thomas, P. J., and Muallem, S. (1999) *J. Biol. Chem.* **274,** 3414–3421
28. Bacic, D., Kaissling, B., McLeroy, P., Zou, L., Baum, M., and Moe, O. W. (2003) *Kidney Int.* **64,** 2133–2141
29. Janecki, A. J., Montrose, M. H., Tse, C. M., de Medina, F. S., Zweibaum, A., and Donowitz, M. (1999) *Am. J. Physiol.* **277,** G292–G305
30. Vachon, P. H., Perreault, N., Magny, P., and Beaulieu, J. F. (1996) *J. Cell Physiol.* **166,** 198–207
31. Saxena, S., Jonsson, Z. O., and Dutta A. (2003) *J. Biol. Chem.* **278,** 44312–44319
32. Hecht, G., Hodges, K., Gill, R. K., Kear, F., Tyagi, S., Malakooti, J., Ramaswamy, K., and Dudeja, P. K. (2004) *Am. J. Physiol.* **287,** G370–G378
33. Bilder, D., and Perrimon, N. (2000) *Nature* **403,** 676–680
34. Gonzalez-Mariscal, L., Betanzos, A., and Avila-Flores, A. (2000) *Semin. Cell Dev. Biol.* **11,** 315–324
35. Lamprecht, G., Weinman, E. J., and Yun, C. H. (1998) *J. Biol. Chem.* **273,** 29972–29978
36. Im, Y. J., Lee, J. H., Park, S. H., Park, S. J., Rho, S. H., Kang, G. B., Kim, E., and Eom, S. H. (2003) *J. Biol. Chem.* **278,** 48099–48104
37. Kurashima, K., Yu, F. H., Cabado, A. G., Szabo, E. Z., Grinstein, S., and Orlowski, J. (1997) *J. Biol. Chem.* **272,** 28672–28679
38. D'Souza, S., Garcia-Cabado, A., Yu, F., Teter, K., Lukacs, G., Skorecki, K., Moore, H. P., Orlowski, J., and Grinstein, S. (1998) *J. Biol. Chem.* **273,** 2035–2043
39. Okamoto, P. M., Gamby, C., Wells, D., Fallon, J., and Vallee, R. B. (2001) *J. Biol. Chem.* **21,** 48458–48465
40. Shibata, T., Chuma, M., Kokubu, A., Sakamoto, M., and Hirohashi S. (2003) *Hepatology* **38,** 178–186
41. Kanai, F., Marignani, P. A., Sarbassova, D., Yagi, R., Hall, R. A., Donowitz, M., Hisaminato, A., Fujiwara, T., Ito, Y., Cantley, L. C., and Yaffe, M. B. (2000) *EMBO J.* **19,** 6778–6791
42. Li, X., Zhang, H., Cheong, A., Leu, S., Chen, Y., Elowsky, C. G., and Donowitz, M. (2004) *J. Physiol.* **556,** 791–804